Radiology: Artificial Intelligence

ORIGINAL RESEARCH

Open Access Data and Deep Learning for Cardiac Device Identification on Standard DICOM and Smartphone-based Chest Radiographs

*Felix Busch, MD** • *Keno K. Bressem, MD** • *Phillip Suwalski, MD* • *Lena Hoffmann, MD* • *Stefan M. Niehues, MD* • *Denis Poddubnyy, MD, MSc* • *Marcus R. Makowski, MD, PhD* • *Hugo J. W. L. Aerts, PhD, MSc* • *Andrei Zhukov, MSc*** • *Lisa C. Adams, MD***

From the Department of Radiology (F.B., L.H., S.M.N.), Department of Anesthesiology, Division of Operative Intensive Care Medicine (F.B.), Department of Cardiology (P.S.), and Department of Rheumatology (K.B.B., D.P., A.Z.), Charité–Universitätsmedizin Berlin, Corporate Member of Freie Universität Berlin and Humboldt Universität zu Berlin, 12203 Berlin, Germany; Department of Radiology and Nuclear Medicine, German Heart Center, Technical University of Munich, Munich, Germany (K.K.B.); Department of Diagnostic and Interventional Radiology, Technical University of Munich, Munich, Germany (F.B., K.K.B., M.R.M., L.C.A.); Artificial Intelligence in Medicine (AIM) Program, Mass General Brigham, Harvard Medical School, Boston, Mass (H.J.W.L.A.); Departments of Radiation Oncology and Radiology, Dana-Farber Cancer Institute and Brigham and Women's Hospital, Boston, Mass (H.J.W.L.A.); and Department of Radiology and Nuclear Medicine, CARIM & GROW, Maastricht University, Maastricht, the Netherlands (H.J.W.L.A.). Received November 9, 2023; revision requested December 18; revision received June 2, 2024; accepted June 25. **Address correspondence to** K.K.B. (email: *keno.bressem@tum.de*).

* F.B. and K.K.B. contributed equally to this work.

** A.Z. and L.C.A. are co–senior authors.

Authors declared no funding for this work.

Conflicts of interest are listed at the end of this article.

See also the commentary by Júdice de Mattos Farina and Celi in this issue.

Radiology: Artificial Intelligence 2024; 6(5):e230502 • https://doi.org/10.1148/ryai.230502 • Content codes: AI CH

Purpose: To develop and evaluate a publicly available deep learning model for segmenting and classifying cardiac implantable electronic devices (CIEDs) on Digital Imaging and Communications in Medicine (DICOM) and smartphone-based chest radiographs.

Materials and Methods: This institutional review board–approved retrospective study included patients with implantable pacemakers, cardioverter defibrillators, cardiac resynchronization therapy devices, and cardiac monitors who underwent chest radiography between January 2012 and January 2022. A U-Net model with a ResNet-50 backbone was created to classify CIEDs on DICOM and smartphone images. Using 2321 chest radiographs in 897 patients (median age, 76 years [range, 18–96 years]; 625 male, 272 female), CIEDs were categorized into four manufacturers, 27 models, and one "other" category. Five smartphones were used to acquire 11 072 images. Performance was reported using the Dice coefficient on the validation set for segmentation or balanced accuracy on the test set for manufacturer and model classification, respectively.

Results: The segmentation tool achieved a mean Dice coefficient of 0.936 (IQR: 0.890–0.958). The model had an accuracy of 94.36% (95% CI: 90.93%, 96.84%; 251 of 266) for CIED manufacturer classification and 84.21% (95% CI: 79.31%, 88.30%; 224 of 266) for CIED model classification.

Conclusion: The proposed deep learning model, trained on both traditional DICOM and smartphone images, showed high accuracy for segmentation and classification of CIEDs on chest radiographs.

Supplemental material is available for this article.

© RSNA, 2024

Cardiac implantable electronic devices (CIEDs), which include implantable cardiac monitors, pacemakers, and implantable cardioverter defibrillators with or without cardiac resynchronization therapy (CRT), have become indispensable tools in the treatment of patients with various cardiac conditions requiring electrical modulation, primary or secondary prevention of sudden cardiac death, or continuous monitoring (1–3). As the worldwide incidence and prevalence of cardiovascular disease continues to rise, the global market for CIEDs is expected to grow dynamically (4–6). In this expanding landscape, clinicians are faced with the imperative task of accurately identifying the manufacturer and specific model of implanted CIEDs. This particularly occurs in emergency scenarios where patient-provided information may be unavailable, but also occurs in everyday clinical practice, such as when information about the CIED is needed during consultation with a cardiologist. While manual algorithms, such as CaRDIA-X, have been effective in identifying CIEDs on chest radiographs, their use can be labor-intensive and time-consuming (7). However, fast and accurate identification can be critical for immediate device interrogation, adjustment of programming parameters, and determination of MRI compatibility (8).

Artificial intelligence algorithms, particularly convolutional neural networks (CNNs), have shown promise in outperforming human performance for CIED identification on chest radiographs (9,10). However, existing studies in this area are limited by a lack of publicly available code and datasets, hindering external testing, transparency,

This copy is for personal use only. To order printed copies, contact reprints@rsna.org

Abbreviations

CIED = cardiac implantable electronic device, CNN = convolutional neural network, CRT = cardiac resynchronization therapy, DICOM = Digital Imaging and Communications in Medicine

Summary

A publicly available, U-Net/ResNet-50 model for identifying cardiac implantable electronic devices on chest radiographs, including smartphone images, showed high segmentation and classification accuracy.

Key Points

- The publicly available deep learning model demonstrated excellent segmentation performance (Dice coefficient: 0.936).
- The model showed high accuracy in classifying cardiac implantable electronic device (CIED) manufacturers (94.36%) and models (84.21%).
- The model's accuracy in CIED identification supports emergency care and illustrates the potential of artificial intelligence in medical imaging, using both standard and smartphone-based image acquisition.

Keywords

Conventional Radiography, Segmentation

reproducibility, and further advancements in the field, such as adaptation to local clinical or business settings (9,11–13). Notably, while one study showcased the feasibility of CNN-based classification of CIED manufacturers using smartphone photographs, simulating a potential use case for a smartphone app that could be used by medical professionals at the bedside, it did not include classification of specific device models, a crucial aspect for clinical application (11).

Addressing the current shortfall in accessible code and datasets, we propose a publicly available deep learning model tailored for CIED chest radiograph segmentation and detailed device classification, compatible with both Digital Imaging and Communications in Medicine (DICOM) and smartphone images. In addition, we provide an open access labeled dataset covering both standard and smartphone images of CIEDs on chest radiographs, aiming to accelerate the development of algorithms capable of precise CIED identification for diverse clinical settings and needs.

Materials and Methods

This retrospective, single-center study received approval from the institutional review board of Charité–Berlin University Medicine (approval no. EA4/042/20) and involved a cohort of adult patients (age ≥ 18 years) with CIEDs. These patients had undergone bedside anterior-posterior or standing posterior-anterior chest radiography within the specified study period from January 2012 to January 2022. Due to the retrospective nature of the study, the requirement for informed consent was waived by the institutional review board. A comprehensive search of the radiology database identified patient records with chest radiograph reports indicating the presence of implantable pacemakers, implantable cardiac defibrillators, CRT devices, or implantable cardiac monitors. Exclusion criteria included images of poor quality, those not capturing the entirety of the devices, and images with multiple devices depicted. In the event of multiple chest radiographs in the same patient, only those taken at distinctly different time points were included. Data extraction was carried out by two independent reviewers (F.B. and P.S., both medical doctors with 4 years of experience in clinical research) who assessed the DICOM images and corresponding medical reports to classify each CIED by manufacturer and model. Discrepancies were resolved by consensus through discussion, ensuring data integrity. The code and dataset are made publicly available *(https://github.com/AndreasZhukov/cied)* (14).

The study did not receive any industry support. All authors had control of the data and the information submitted for publication.

Dataset and Preprocessing

In compliance with privacy regulations, all DICOM images were anonymized by deleting the header information and using object character recognition software (pytesseract; *https://pypi.org/project/pytesseract/*) to remove any burned-in text. These images were then converted to PNG format. Three authors (F.B., a medical doctor with 4 years of clinical research experience in radiology, and K.K.B. and L.C.A., two board-certified radiologists with 7 and 8 years of radiology reading experience, respectively) then photographed the chest radiographs with one of five different smartphone models, capturing images from a clinical monitor at different angles to mimic real-world viewing conditions and provide a variety of image qualities for analysis. To avoid overrepresentation of patients, they were divided into three groups, with each author photographing the patients in one group. This method ensured that every patient was included in only one group, minimizing potential biases from variations in the number of images per device or patient. The entire collection, encompassing smartphone-captured and digitally converted images, will be made accessible on PhysioNet for broader research purposes. To prepare the data for segmentation modeling, reference standard annotations of CIEDs were manually delineated by two board-certified radiologists (K.K.B. and L.C.A.), both with substantial expertise in diagnostic imaging and image processing. Inconsistencies were reconciled through a consensus reached after thorough and critical discussion. The readers employed 3D Slicer (15) for annotation, ensuring precise and accurate outlines for the subsequent segmentation tasks. The preprocessing pipeline involved rescaling the images to a consistently smaller dimension, adhering to the original aspect ratio, and then center cropping to square frames. The input for the classification models was the cropped largest connected region. A split of 70% training and 30% validation sets was adopted for the segmentation model, while a 70%:20%:10% split was used for the training, validation, and testing datasets of the classification models. We opted for a larger validation set compared with the test set to allow for more comprehensive hyperparameter tuning and model selection during the training process. The splits included both DICOM and smartphone images. However, due to the variable number of DICOM and smartphone images per patient and the uneven distribution of devices, our final split deviated

slightly from a standard 70%:20%:10% distribution, resulting in 70.03% for training, 18.52% for validation, and 11.45% for testing (see also Appendix S1). To ensure a robust representation in the model, classes with fewer than 20 original images were grouped into an "other" category.

Model Training and Postprocessing

Model training incorporated a U-Net architecture with a ResNet-50 backbone for image segmentation and a ResNet-50 for classification. The segmentation model was used as a preprocessing step for the classification models. Creating segmentations of the CIED allowed the images to be cropped to just the CIED before the classification step, greatly reducing the variability and size of the classification model's input. The training was conducted on a Linux Ubuntu 18.04 machine with a dedicated NVIDIA GTX 2080Ti GPU, utilizing the Python programming language (version 3.8.16) and the FastAi library (version 2.4; *https://docs.fast.ai/*). The model was fed random 256 × 256-pixel patches of the original images, with applied data augmentation techniques including random rotations (up to ± 30°) and horizontal flipping (50% probability), to improve the model's ability to generalize. The initial hyperparameters were manually set based on our experience and best practices in the field. We then performed a grid search to find the optimal hyperparameters for the segmentation and classification models. Final hyperparameters were a batch size of 32, learning rate of 1e-3, weight decay of 1e-5, Adam optimizer, and 50 epochs of training. Please refer to Figure 1 for a schematic illustration of the data pipeline, model architecture, and classification models.

Statistical Analysis

Statistical analyses were performed using R software (version 4.3.1; R Foundation for Statistical Computing), with the tidyverse, pROC, and caret packages (16–19). The performance of the segmentation model was evaluated using the Dice coefficient and IQR reported as Q1–Q3 on the validation dataset. In addition, detection accuracy was calculated based on the threshold of 25% or more versus less than 25% of the image crop containing the CIED of interest. For the classification model, accuracy and 95% CIs were calculated for each CIED manufacturer and model within the test datasets. Additionally, confusion matrices were constructed to facilitate a more detailed performance assessment. A comprehensive array of diagnostic and performance metrics—including sensitivity, specificity, positive predictive value, negative predictive value, precision, recall, F1 score, prevalence, detection rate, and detection prevalence—were calculated to assess the classification model's efficacy.

External Testing

For external testing, we identified two publications: one offering a dataset and web application for CIED manufacturer and model group classification and another providing a smartphone application for manufacturer classification only (9,11). Both applications were evaluated on our test dataset. A subset of 15 external test set images from Howard et al (9) containing CIED manufacturers and models presented in our training data were used for external testing of our algorithm. A detailed description of the external comparison process is provided in Appendix S2.

Results

Dataset Composition

Upon comprehensive examination of our local database, we extracted 2321 DICOM images in 897 patients that were suitable for analysis from an initial pool of 2401 (see Fig 2), following the exclusion of 80 images because of incompletely captured devices (2.12%, 51 of 2401), the presence of multiple CIEDs on one image (0.83%, 20 of 2401), or insufficient image quality (0.37%, nine of 2401). Examples of chest radiographs excluded because of poor quality are presented in Figure S1.

The included images spanned across four manufacturers and were further categorized into 27 distinct CIED models (89.92%, 2087 of 2321) and a collective other category for less represented models (10.08%, 234 of 2321). Device manufacturer and model information were extracted from electronic medical records, correlating radiographic features in DICOM images with documented device details. This ensured accurate data representation and integrity. Regarding patient demographics, the study cohort had a median age of 76 years (range, 18–96 years), and the majority of patients were male (69.67%, 625 of 897).

The photographic database, which was intended to simulate a realistic clinical environment, consisted of 11 072 images. These were distributed among five different smartphone cameras, thereby introducing a range of image acquisition variables. The distribution was as follows: iPhone 13 mini (6.28%, 695 of 11 072), Samsung Galaxy S4 (15.13%, 1675 of 11 072), iPhone 8 (26.10%, 2890 of 11 072), iPhone 13 (26.21%, 2902 of 11 072), and Samsung Galaxy S5 (26.28%, 2910 of 11 072) (see detailed breakdown in Table S1). This diversity in the image acquisition process was designed to challenge the robustness of our models in varying conditions reflective of bedside clinical settings.

Please refer to Table 1 to view the total list of CIED manufacturers and models, including the number of DICOM images in total and in the training, validation, and test datasets.

Model Performance

Segmentation and classification efficacy.— The segmentation model achieved an average Dice coefficient of 0.936 (IQR: 0.890–0.958) on the validation set. The highest Dice coefficient was achieved for CIEDs from Vitatron (0.955 [IQR: 0.917–0.936]), followed by Biotronik (0.943 [IQR: 0.915–0.954]), Medtronic (0.940 [IQR: 0.906–0.958]), Boston Scientific (0.930 [IQR: 0.865–0.964]), and Abbott Laboratories/St. Jude Medical (0.870 [IQR: 0.709–0.942]). In our test set, two devices were not detected, resulting in an accuracy of 99.27% (95% CI: 97.21%, 99.98%; 273 of 275) for our segmentation

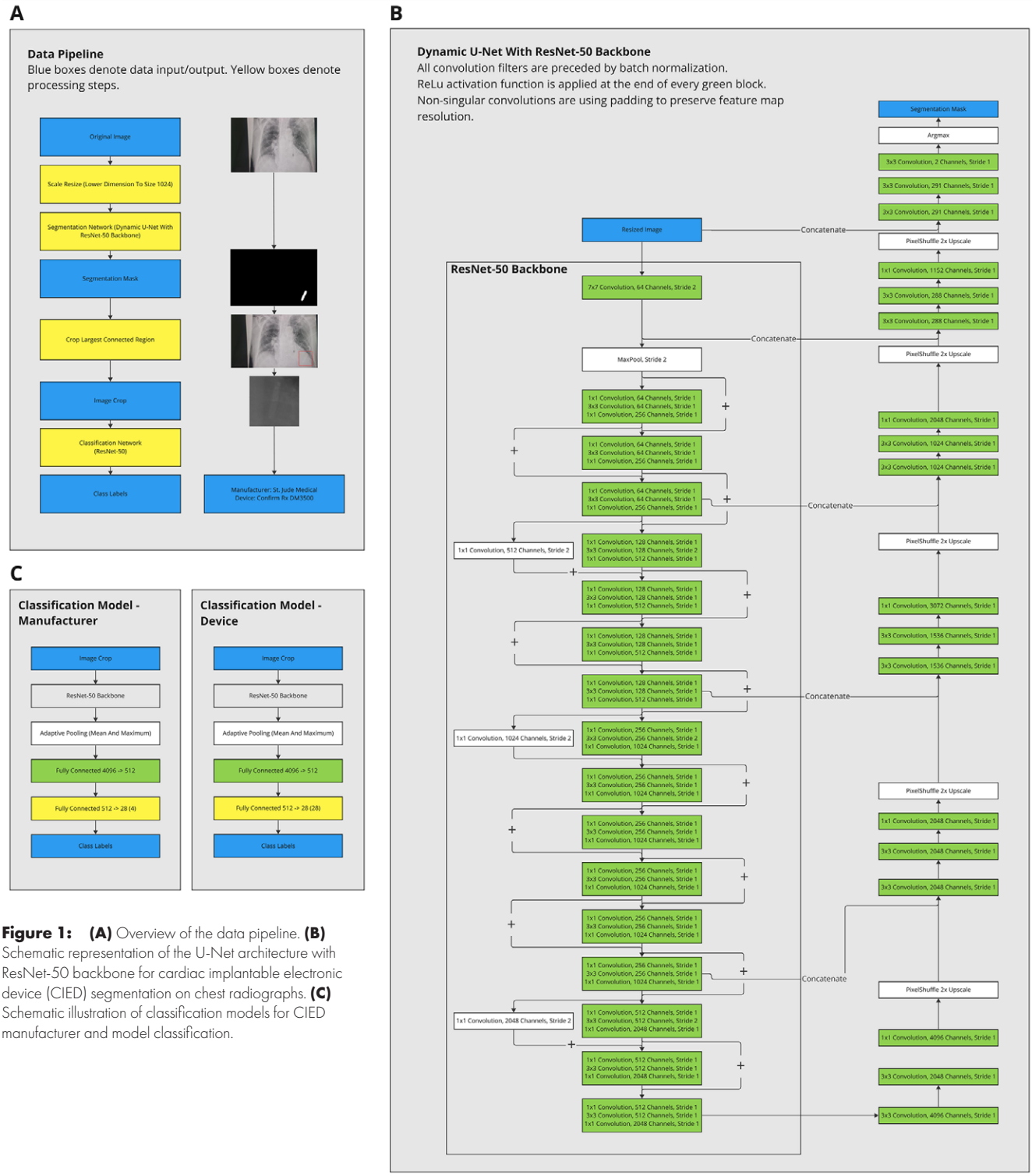


Figure 1: **(A)** Overview of the data pipeline. **(B)** Schematic representation of the U-Net architecture with ResNet-50 backbone for cardiac implantable electronic device (CIED) segmentation on chest radiographs. **(C)** Schematic illustration of classification models for CIED manufacturer and model classification.

model in detecting CIEDs. The classification models reached an overall accuracy of 94.36% (95% CI: 90.93%, 96.84%; 251 of 266) for CIED manufacturer and 84.21% (95% CI: 79.31%, 88.30%; 224 of 266) for model classification on the test set. Detailed performance metrics of the classification model for each CIED manufacturer and model are reported in Table 2, while the performance comparison between original DICOM and smartphone images in the test set is shown in Table 3. Confusion matrices for manufacturer and model classifications are displayed in Figure 3, indicating a higher performance in manufacturer classification compared with the model classification, aligning with the anticipated complexity of the latter task.

External comparison.— The web application of Howard et al (9) achieved an accuracy of 96.97% (32 of 33) for manufac-

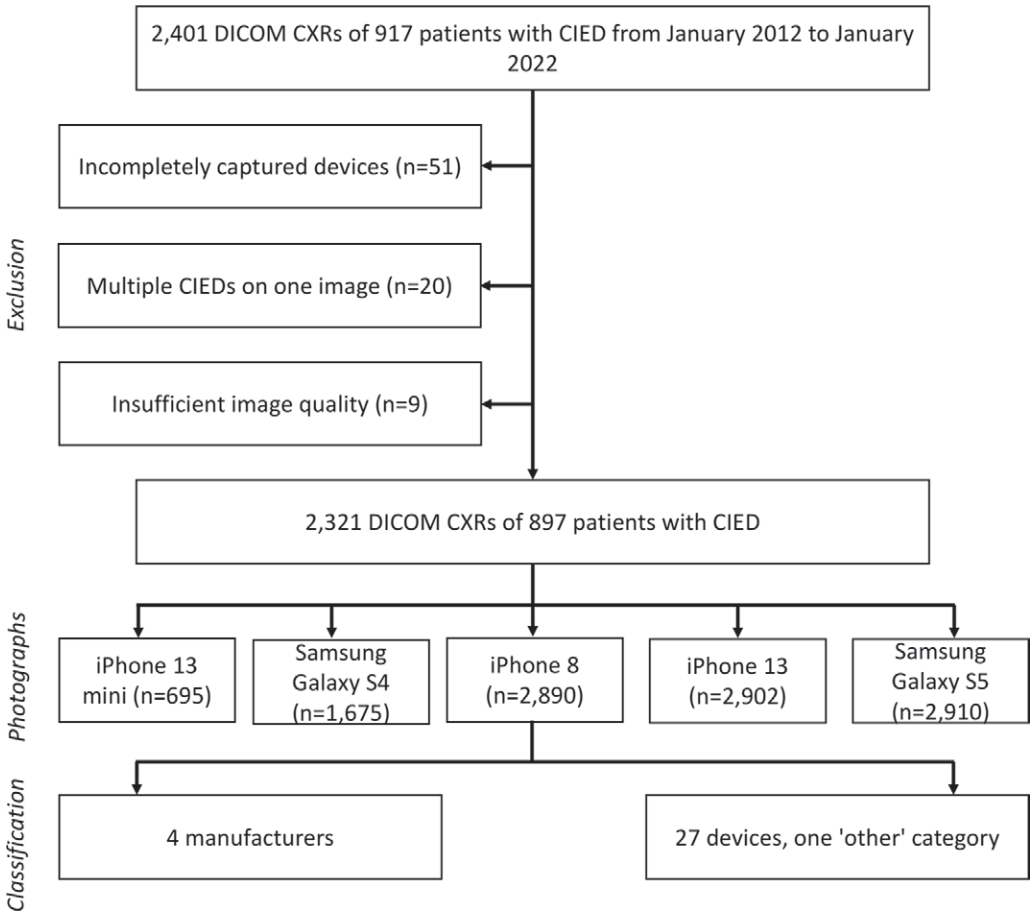


Figure 2: Flow diagram depicts study exclusion criteria and study design. CIED = cardiac implantable electronic device, CXR = chest radiograph, DICOM = Digital Imaging and Communications in Medicine.

turer classification and 90.91% (30 of 33) for model group classification on 33 selected images in our test set. When evaluating our algorithm on 15 test data images from Howard et al containing CIED manufacturers and models presented in our training data, our model achieved an accuracy of 100.00% (15 of 15) for CIED manufacturer classification and 86.67% (13 of 15) for CIED model group classification. The smartphone application by Weinreich et al (11) achieved an accuracy of 67.27% (185 of 275) for CIED manufacturer classification on our test set, which included only original images to avoid multiplicative errors of photographing a photograph. The detailed comparison can be found in Appendix S2.

Discussion

The integration of artificial intelligence into medical imaging promises to improve clinical care. In this study, we present a deep learning model designed to segment CIEDs and classify CIED manufacturers and exact models using both traditional DICOM chest radiographs and smartphone images. Our model achieved a Dice coefficient of 0.936 for CIED segmentation and accuracies of 94.36% and 84.21% for manufacturer and model classification, respectively, on the test set.

Compared with prior studies, we have incorporated a diverse range of smartphone images in addition to DICOM images for model training and validation, making our approach more robust and applicable to real-world scenarios. Second, our model provides a more granular classification of CIEDs by identifying the exact models, which we believe to be more clinically relevant than the model group classification used in previous studies (9,11–13). Third, we have made our dataset and code publicly available, encouraging further research and collaborations in this field. Table 4 provides an overview of previously published deep learning models for the classification of CIEDs on chest radiographs compared with our proposed model.

Howard et al (2019) (9) evaluated the DenseNet, Inception V3, VGGNet, ResNet, and Xception architectures for the classification of five CIED manufacturers and 45 model groups, using a dataset of 1676 DICOM images from a single institution in the United Kingdom, with the Xception architecture achieving the highest accuracy on the test set in classifying manufacturers (99.60%) and model groups (96.40%). As the test dataset was available, we compared our model on a subset of test data images from Howard et al (9), achieving a comparable accuracy for both manufacturer and model group classification despite the limitation that our approach was designed to classify the exact CIED models. Parallel to the study of Howard et al (9), Kim et al (13) presented a CNN architecture that integrates a class-independent CIED detector based on the MobileNet architecture and a multitask learner

Table 1: List of Manufacturers, Devices, and Categories in Total and Divided into Training, Validation, and Test Datasets

Manufacturer/Device	Total	Training Dataset	Validation Dataset	Test Dataset	Device Category
Medtronic, all devices	1218	849	240	129	…
Attesta DR MRI SureScan	263	186	51	26	Dual-chamber PM
Mirro MRI VR SureScan	237	168	45	24	Single-chamber ICD
Reveal LINQ	94	69	16	9	ICM
Serena Quad CRT-P MRI SureScan	77	52	17	8	CRT-P
Compia MRI Quad CRT-D SureScan	51	36	9	6	CRT-D
Ensura DR MRI SureScan	39	22	10	7	Dual-chamber PM
Reveal XT	31	19	7	5	ICM
Q20 SR MRI SureScan	342	238	71	33	Single-chamber PM
Other	84	59	14	11	…
Biotronik, all devices	517	373	77	67	…
Enticos 4 DR	111	76	26	9	Dual-chamber PM
Enticos 4 SR	48	38	6	4	Single-chamber PM
Enitra 8 HF-T QP	79	60	10	9	CRT-P
Ilivia 7 VR-T	34	24	5	5	Single-chamber ICD
Ilivia 7 HF-T QP	22	17	3	2	CRT-D
Ecuro SR-T	29	20	4	5	Single-chamber ICD
Rivacor 7 HF-T QP	25	17	3	5	CRT-D
Rivacor 5 VR-T DX	34	21	5	8	Single-chamber ICD
Etrinsa 8 HF-T	22	15	2	5	CRT-P
Enitra 6 DR-T	20	15	3	2	Dual-chamber PM
Other	93	70	10	13	…
Abbott Laboratories (including St. Jude Medical), all devices	401	279	78	44	…
Confirm Rx DM3500	137	90	32	15	ICM
Ellipse VR	97	64	23	10	Single-chamber ICD
Quadra Allure MP	84	63	12	9	CRT-P
Quadra Assura MP	39	28	5	6	CRT-D
SJM Confirm	26	20	5	1	ICM
Other	18	14	1	3	…
Boston Scientific, all devices	185	124	35	26	…
Charisma ×4 CRT-D	64	44	12	8	CRT-D
Valitude ×4 CRT-P	32	19	7	6	CRP-P
Inogen EL ICD VR	27	19	3	5	Single-chamber ICD
Origen Mini ICD	23	14	4	5	Single-chamber ICD
Other	39	28	9	2	…
Other devices total	234	171	34	29	…

Note.—Unless otherwise indicated, data are numbers of devices. CRT-D = cardiac resynchronization therapy defibrillator, CRT-P = cardiac resynchronization therapy pacemaker, ICD = implantable cardioverter defibrillator, ICM = implantable cardiac monitor, PM = pacemaker.

using the DenseNet backbone for CIED classification. Using a dataset of 9912 DICOM images, including four CIED manufacturers and 26 model groups from two Korean institutions, this approach achieved an accuracy of 95.80% for manufacturer and 85.40% for model group classification on the external test dataset (13). Although the results for manufacturer classification are comparable to those of our study, the approaches by Howard et al (9) and Kim et al (13) differ from ours by focusing on model group classification (ie, a common series of CIEDs by one manufacturer, without classifying the exact models, including the specific name, generation, and category of each CIED). This approach poses limitations, such as different CIED categories being classified together (eg, the Quadra series from Abbott Laboratories [formerly St. Jude Medical], where Quadra Allure MP is a CRT pacemaker and Quadra Assura MP a CRT defibrillator) or disparities in MRI compatibility between different device generations (9,11).

To date, only one study has developed a deep learning approach for specific model classification: Theriault Lauzier et al (12) used

Table 2: Performance Metrics across Datasets

Manufacturer/Device	Sensitivity (%)	Specificity (%)	PPV (%)	NPV (%)	F1 Score	Detection Rate (%)	Detection Prevalence (%)	Accuracy (%)	Balanced Accuracy (%)
Medtronic, all devices	93.80 (121/129)	96.35 132/137)	96.03 (121/126)	94.29 (132/140)	0.949	48.50 (129/266)	45.49 (121/266)	95.11 (253/266)	95.10
Attesta DR MRI surescan	100.00 (26/26)	100.00 (240/240)	100.00 (26/26)	100.00 (240/240)	1.000	9.77 (26/266)	9.77 (26/266)	100.00 (266/266)	100.00
Mirro MRI VR surescan	91.67 (22/24)	97.52 (236/242)	78.57 (22/28)	99.16 (236/238)	0.846	9.02 (24/266)	8.27 (22/266)	97.00 (258/266)	94.57
Reveal LINQ	44.44 (4/9)	98.83 (254/257)	57.14 (4/7)	98.07 (254/259)	0.500	3.38 (9/266)	1.50 (4/266)	97.00 (258/266)	71.56
Serena Quad CRT-P MRI SureScan	100.00 (8/8)	99.61 (257/258)	88.89 (8/9)	100.00 (257/257)	0.941	3.01 (8/266)	3.01 (8/266)	99.62 (265/266)	99.80
Compia MRI Quad CRT-D SureScan	83.33 (5/6)	98.85 (257/260)	62.50 (5/8)	99.61 (257/258)	0.714	2.26 (6/266)	1.88 (5/266)	98.50 (262/266)	91.10
Ensura DR MRI SureScan	85.71 (6/7)	100.00 (259/259)	100.00 (6/6)	99.62 (259/260)	0.923	2.63 (7/266)	2.26 (6/266)	99.62 (265/266)	92.90
Reveal XT	60.00 (3/5)	100.00 (261/261)	100.00 (3/3)	99.24 (261/263)	0.750	1.88 (5/266)	1.13 (3/266)	99.25 (264/266)	80.00
Q20 SR MRI SureScan	93.94 (31/33)	99.14 (231/233)	93.94 (31/33)	99.14 (231/233)	0.939	12.41 (33/266)	11.65 (31/266)	98.50 (262/266)	96.52
Biotronik, all devices	92.54 (62/67)	98.00 (195/199)	93.94 (62/66)	97.50 (195/200)	0.932	25.19 (67/266)	23.31 (62/266)	96.62 (257/266)	95.34
Enticos 4 DR	100.00 (9/9)	99.61 (256/257)	90.00 (9/10)	100.00 (256/256)	0.947	3.38 (9/266)	3.38 (9/266)	99.62 (265/266)	99.80
Enticos 4 SR	75.00 (3/4)	99.62 (261/262)	75.00 (3/4)	99.62 (261/262)	0.75	1.50 (4/266)	1.13 (3/266)	99.25 (264/266)	87.30
Enitra 8 HF-T QP	77.78 (7/9)	100.00 (257/257)	100.00 (7/7)	99.23 (257/259)	0.875	3.38 (9/266)	2.63 (7/266)	99.25 (264/266)	88.90
Ilivia 7 VR-T	80.00 (4/5)	98.85 (258/261)	57.14 (4/7)	99.61 (258/259)	0.667	1.88 (5/266)	1.50 (4/266)	98.50 (262/266)	89.40
Ilivia 7 HF-T QP	100.00 (2/2)	100.00 (264/264)	100.00 (2/2)	100.00 (264/264)	1.000	0.75 (2/266)	0.75 (2/266)	100.00 (266/266)	100.00
Ecuro SR-T	60.00 (3/5)	100.00 (261/261)	100.00 (3/3)	99.24 (261/263)	0.75	1.88 (5/266)	1.13 (3/266)	99.25 (264/266)	80.00
Rivacor 7 HF-T QP	80.00 (4/5)	99.62 (260/261)	80.00 (4/5)	99.62 (260/261)	0.8	1.88 (5/266)	1.50 (4/266)	99.25 (264/266)	89.76
Rivacor 5 VR-T DX	50.00 (4/8)	100.00 (258/258)	100.00 (4/4)	98.47 (258/262)	0.667	3.01 (8/266)	1.50 (4/266)	98.50 (262/266)	75.00
Etrinsa 8 HF-T	100.00 (5/5)	100.00 261/261)	100.00 (5/5)	100.00 (261/261)	1.000	1.88 (5/266)	1.88 (5/266)	100.00 (266/266)	100.00
Enitra 6 DR-T	50.00 (1/2)	100.00 (264/264)	100.00 (1/1)	99.62 (264/265)	0.667	0.75 (2/266)	0.38 (1/266)	99.62 (265/266)	75.00
Abbott Laboratories (including St. Jude Medical), all devices	95.45 (42/44)	97.30 (216/222)	87.50 (42/48)	99.08 (216/218)	0.913	16.54 (44/266)	15.79 (42/266)	97.00 (258/266)	96.39
Confirm Rx DM3500	100.00 (15/15)	98.80 (248/251)	83.33 (15/18)	100.00 (248/248)	0.909	5.64 (15/266)	5.64 (15/266)	98.87 (263/266)	99.40
Ellipse VR	100.00 (10/10)	99.61 (255/256)	90.91 (10/11)	100.00 (255/255)	0.952	3.76 (10/266)	3.76 (10/266)	99.62 (265/266)	99.80
Quadra Allure MP	100.00 (9/9)	99.22 (255/257)	81.82 (9/11)	100.00 (255/255)	0.900	3.38 (9/266)	3.38 (9/266)	99.25 (264/266)	99.61

(Table 2 continues)

Table 2 *(continued)*: Performance Metrics across Datasets

Manufacturer/Device	Sensitivity (%)	Specificity (%)	PPV (%)	NPV (%)	F1 Score	Detection Rate (%)	Detection Prevalence (%)	Accuracy (%)	Balanced Accuracy (%)
Quadra Assura MP	100.00 (6/6)	100.00 (260/260)	100.00 (6/6)	100.00 (260/260)	1.000	2.26 (6/266)	2.26 (6/266)	100.00 (266/266)	100.00
SJM Confirm	100.00 (1/1)	100.00 (265/265)	100.00 (1/1)	100.00 (265/265)	1.000	0.38 (1/266)	0.38 (1/266)	100.00 (266/266)	100.00
Boston Scientific, all devices	100.00 (26/26)	100.00 (240/240)	100.00 (26/26)	100.00 (240/240)	1.000	9.77 (26/266)	9.77 (26/266)	100.00 (266/266)	100.00
Charisma ×4 CRT-D	87.50 (7/8)	100.00 (258/258)	100.00 (7/7)	99.61 (258/259)	0.933	3.01 (8/266)	2.63 (7/266)	99.62 (265/266)	93.77
Valitude ×4 CRT-P	100.00 (6/6)	100.00 (260/260)	100.00 (6/6)	100.00 (260/260)	1.000	2.26 (6/266)	2.26 (6/266)	100.00 (266/266)	100.00
Inogen EL ICD VR	60.00 (3/5)	99.23 (259/261)	60.00 (3/5)	99.23 (259/261)	0.600	1.88 (5/266)	1.13 (3/266)	98.50 (262/266)	79.61
Origen Mini ICD	100.00 (5/5)	100.00 (261/261)	100.00 (5/5)	100.00 (261/261)	1.000	1.88 (5/266)	1.88 (5/266)	100.00 (266/266)	100.00
Other devices total	51.72 (15/29)	94.51 (224/237)	53.57 (15/28)	94.12 (224/238)	0.526	10.90 (29/266)	5.64 (15/266)	89.85 (239/266)	73.10

Note.—Data in parentheses are numerators and denominators. CRT-D = cardiac resynchronization therapy defibrillator, CRT-P = cardiac resynchronization therapy pacemaker, ICD = implantable cardioverter defibrillator, ICM = implantable cardiac monitor, NPV = negative predictive value, PM = pacemaker, PPV = positive predictive value.

Table 3: Comparison of Classification Performance on DICOM versus Smartphone Images in Test Set

Manufacturer/Device	Test Dataset*	Sensitivity (%)		Specificity (%)		Accuracy (%)	
		Originals	Photos	Originals	Photos	Originals	Photos
Medtronic, all devices	129	93.80 (121/129)	93.80 (121/129)	96.35 (132/137)	93.43 (128/137)	95.11 (253/266)	93.60 (249/266)
Attesta DR MRI SureScan	26	100.00 (26/26)	96.15 (25/26)	100.00 (240/240)	99.58 (239/240)	100.00 (266/266)	99.25 (264/266)
Mirro MRI VR SureScan	24	91.67 (22/24)	95.83 (23/24)	97.52 (236/242)	97.93 (237/242)	96.99 (258/266)	97.74 (260/266)
Reveal LINQ	9	44.44 (4/9)	88.89 (8/9)	98.83 (254/257)	98.83 (254/257)	96.99 (258/266)	98.50 (262/266)
Serena Quad CRT-P MRI SureScan	8	100.00 (8/8)	100.00 (8/8)	99.61 (257/258)	99.61 (257/258)	99.62 (265/266)	99.62 (265/266)
Compia MRI Quad CRT-D SureScan	6	83.33 (5/6)	66.67 (4/6)	98.85 (257/260)	98.46 (256/260)	98.50 (262/266)	97.74 (260/266)
Ensura DR MRI SureScan	7	85.71 (6/7)	57.14 (4/7)	100.00 (259/259)	100.00 (259/259)	99.62 (265/266)	98.87 (263/266)
Reveal XT	5	60.00 (3/5)	80.00 (4/5)	100.00 (261/261)	100.00 (261/261)	99.25 (264/266)	99.62 (265/266)
Q20 SR MRI SureScan	33	93.94 (31/33)	90.91 (30/33)	99.14 (231/233)	99.14 (231/233)	98.50 (262/266)	98.12 (261/266)
Other	11						
Biotronik, all devices	67	92.54 (62/67)	94.03 (63/67)	97.99 (195/199)	96.98 (193/199)	96.62 (257/266)	96.24 (256/266)
Enticos 4 DR	9	100.00 (9/9)	100.00 (9/9)	99.61 (256/257)	99.22 (255/257)	99.62 (265/266)	99.25 (264/266)
Enticos 4 SR	4	75.00 (3/4)	100.00 (4/4)	99.62 (261/262)	99.62 (261/262)	99.25 (264/266)	99.62 (265/266)
Enitra 8 HF-T QP	9	77.78 (7/9)	77.78 (7/9)	100.00 (257/257)	99.61 (256/257)	99.25 (264/266)	98.87 (263/266)

(Table 3 continues)

Table 3 (*continued*): Comparison of Classification Performance on DICOM versus Smartphone Images in Test Set

Manufacturer/Device	Test Dataset*	Sensitivity (%)		Specificity (%)		Accuracy (%)	
		Originals	Photos	Originals	Photos	Originals	Photos
Ilivia 7 VR-T	5	80.00 (4/5)	100.00 (2/2)	98.85 (258/261)	99.62 (263/264)	98.50 (262/266)	99.62 (265/266)
Ilivia 7 HF-T QP	2	100.00 (2/2)	100.00 (5/5)	100.00 (264/264)	99.62 (260/261)	100.00 (266/266)	99.62 (265/266)
Ecuro SR-T	5	60.00 (3/5)	60.00 (3/5)	100.00 (261/261)	100.00 (261/261)	99.25 (264/266)	99.25 (264/266)
Rivacor 7 HF-T QP	5	80.00 (4/5)	80.00 (4/5)	99.62 (260/261)	98.85 (258/261)	99.25 (264/266)	98.50 (262/266)
Rivacor 5 VR-T DX	8	50.00 (4/8)	50.00 (4/8)	100.00 (258/258)	99.61 (257/258)	98.50 (262/266)	98.12 (261/266)
Etrinsa 8 HF-T	5	100.00 (5/5)	100.00 (5/5)	100.00 (261/261)	100.00 (261/261)	100.00 (266/266)	100.00 (266/266)
Enitra 6 DR-T	2	50.00 (1/2)	0.00 (0/2)	100.00 (264/264)	100.00 (264/264)	99.62 (265/266)	99.25 (264/266)
Other	13						
Abbott Laboratories (including St. Jude Medical), all devices	44	95.45 (42/44)	84.09 (37/44)	97.30 (216/222)	98.20 (218/222)	96.99 (258/266)	95.86 (255/266)
Confirm Rx DM3500	15	100.00 (15/15)	93.33 (14/15)	98.80 (248/251)	99.60 (250/251)	98.87 (263/266)	99.25 (264/266)
Ellipse VR	10	100.00 (10/10)	90.00 (9/10)	99.61 (255/256)	100.00 (256/256)	99.62 (265/266)	99.62 (265/266)
Quadra Allure MP	9	100.00 (9/9)	100.00 (9/9)	99.22 (255/257)	100.00 (257/257)	99.25 (264/266)	100.00 (266/266)
Quadra Assura MP	6	100.00 (6/6)	83.33 (5/6)	100.00 (260/260)	100.00 (260/260)	100.00 (266/266)	99.62 (265/266)
SJM Confirm	1	100.00 (1/1)	100.00 (1/1)	100.00 (265/265)	100.00 (265/265)	100.00 (266/266)	100.00 (266/266)
Other	3						
Boston Scientific, all devices	26	100.00 (26/26)	100.00 (26/26)	100.00 (240/240)	100.00 (240/240)	100.00 (266/266)	100.00 (266/266)
Charisma ×4 CRT-D	8	87.50 (7/8)	75.00 (6/8)	100.00 (258/258)	100.00 (258/258)	99.62 (265/266)	99.25 (264/266)
Valitude ×4 CRT-P	6	100.00 (6/6)	100.00 (6/6)	100.00 (260/260)	100.00 (260/260)	100.00 (266/266)	100.00 (266/266)
Inogen EL ICD VR	5	60.00 (3/5)	80.00 (4/5)	99.23 (259/261)	99.23 (259/261)	98.50 (262/266)	98.87 (263/266)
Origen Mini ICD	5	100.00 (5/5)	100.00 (5/5)	100.00 (261/261)	100.00 (261/261)	100.00 (266/266)	100.00 (266/266)
Other	2						
Other devices total	29	51.72 (15/29)	51.72 (15/29)	94.51 (224/237)	94.09 (223/237)	89.85 (239/266)	89.47 (238/266)

Note.—Data in parentheses are numerators and denominators. CRT-D = cardiac resynchronization therapy defibrillator, CRT-P = cardiac resynchronization therapy pacemaker, ICD = implantable cardioverter defibrillator, ICM = implantable cardiac monitor.
* Data are numbers of devices.

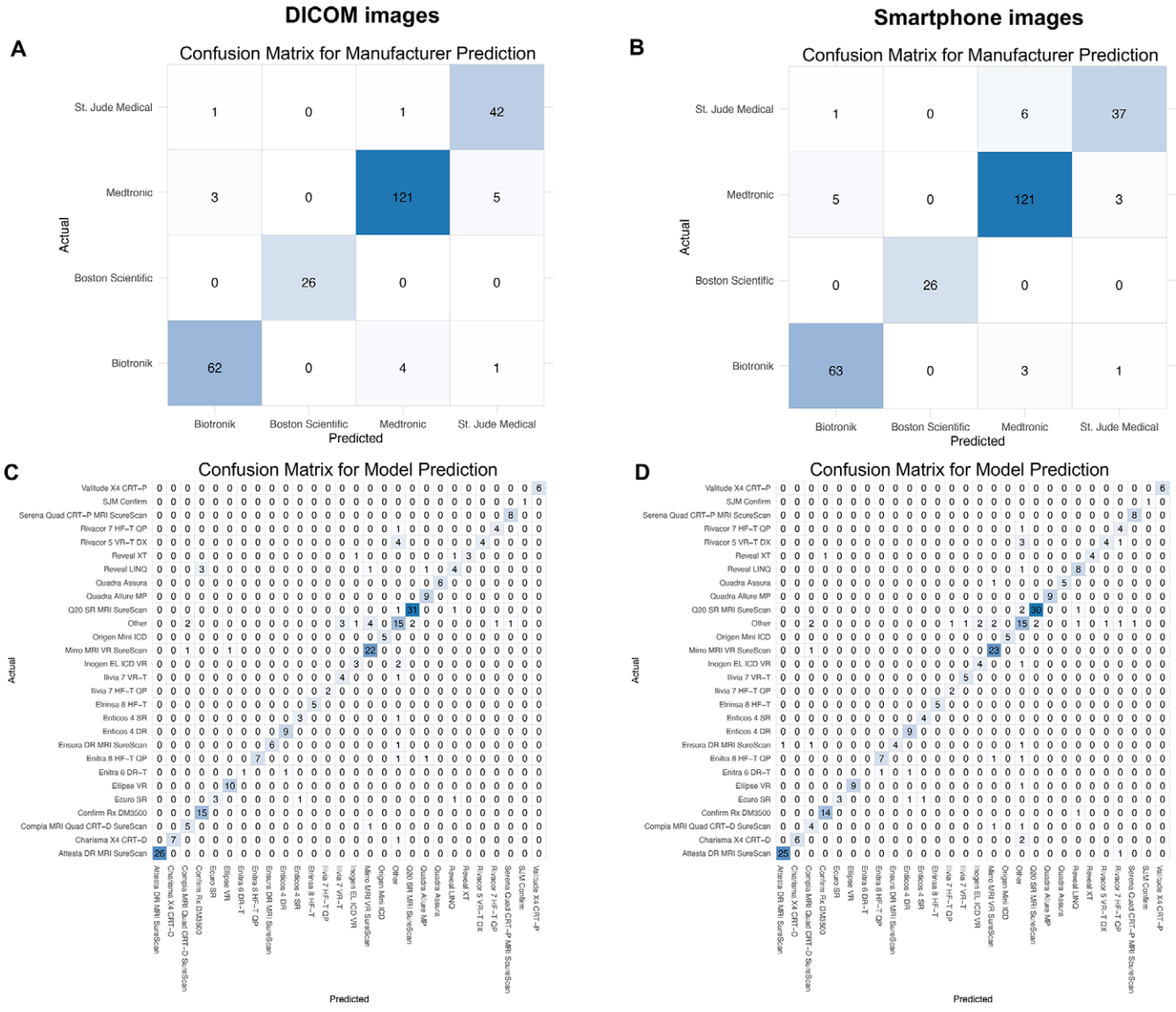


Figure 3: Confusion matrices for cardiac implantable electronic device manufacturer and model classification on original DICOM images (**A**, manufacturer; **C**, model) and smartphone images (**B**, manufacturer; **D**, model). DICOM = Digital Imaging and Communications in Medicine.

the Faster *R*-CNN with a ResNet152 backbone for device detection and the Xception model for the classification of eight CIED manufacturers and 307 specific models on a dataset of 102749 DICOM images from two Canadian institutions, achieving an accuracy of 99.50% for manufacturer classification and 75.00% for exact model classification on the validation set. Although the specific model classification was performed on a higher number of images, the accuracy was lower compared with our study, possibly due to the higher number of specific CIED models classified with varying sample sizes and device characteristics. Furthermore, the lack of a separate test set in their study may lead to an overestimation of the model's performance and reduce its generalizability when applied to unseen real-world data.

Finally, only one study focused on developing a deep learning algorithm for CIED manufacturer classification using a smartphone app, providing a clinically applicable bedside approach (11). Comprising a dataset of 1509 chest radiographs from a single institution in the United States and 3008 smartphone images, Weinreich et al (11) reported an accuracy of 97.00% for manufacturer classification on the test set. Although smartphone photographs were used for model training in this study, only CIED manufacturers and not model groups or specific models were classified. In contrast, our model was trained on a higher number of DICOM images and smartphone photographs and included the manufacturer and exact model classification. This likely contributed to the lower performance of the smartphone application when applied to our test set, achieving an accuracy of 67.30% for CIED manufacturer classification.

Our study had some limitations. Most importantly, as a single-center study with 897 patients, our dataset did not provide an exhaustive catalog of device manufacturers and models used in other geographic regions. Additionally, the data used presented an uneven distribution across various CIED models and manufacturers. To address this disparity and mitigate the risk of incorrect classification, our approach classified less prevalent models as other. Future studies should aim to include a wider

Table 4: Proposed Model Compared with Published Deep Learning Algorithms for Classification of Cardiac Implantable Electronic Devices on Chest Radiographs

			Dataset Composition								Classification Accuracy (%)		
Architecture	Dataset Available	Code Available	Smartphone Photographs	DICOM Images	Manufacturers	All CEIDs	Pacemakers	ICDs	CRTs	ICMs	Manufacturers	Model Groups	Exact Model
CNN (proposed model)	Yes	Yes	11 072	2321	4	27	6	7	10	4	94.36	NA	84.21
CNN (9)	Yes	No	NA	1676	5	64	37	10	15	2	99.60	96.40	NA
CNN (11)	No	No	3008	1509	4	NA	NA	NA	NA	NA	97.00	NA	NA
CNN (12)	No	No	NA	102 749	8	307	NA	NA	NA	NA	99.50*	NA	75.00*
CNN (13)	No	No	NA	9912	4	26†	14†	4†	8†	0†	95.80	85.40	NA

Note.—Unless otherwise indicated, data are numbers. CEID = cardiac implantable electronic device, CNN = convolutional neural network, CRT = cardiac resynchronization therapy, DICOM = Digital Imaging and Communications in Medicine, ICD = implantable cardioverter defibrillator, ICM = implantable cardiac monitor, NA = not available.

* No test dataset was used, and accuracy was reported on the validation dataset.

† Reported as model groups.

variety of device manufacturers and models from multiple centers to improve the generalizability of the models.

In conclusion, our study demonstrates the feasibility and potential of using deep learning models for CIED identification on chest radiographs, including smartphone images. The publicly available dataset and code provided in this study can serve as a valuable resource for further research and development in this field, ultimately leading to improved patient care and management.

Acknowledgments: K.K.B. is grateful for his participation in the Berlin Institute of Health (BIH) Charité Digital Clinician Scientist Program, funded by the Charité–Universitätsmedizin Berlin and the BIH.

Author contributions:: Guarantors of integrity of entire study, **F.B., K.K.B.**; study concepts/study design or data acquisition or data analysis/interpretation, all authors; manuscript drafting or manuscript revision for important intellectual content, all authors; approval of final version of submitted manuscript, all authors; agrees to ensure any questions related to the work are appropriately resolved, all authors; literature research, **F.B., P.S., L.H., S.M.N.**; clinical studies, **F.B., K.K.B., P.S., L.H.**; experimental studies, **K.K.B., P.S.**; statistical analysis, **F.B., K.K.B., A.Z.**; and manuscript editing, all authors

Disclosures of conflicts of interest: **F.B.** No relevant relationships. **K.K.B.** Grant from the European Union (101079894) and Wilhelm Sander Foundation; research grant for the COMFORT Project (EU Horizon 2020); speaker fees for Canon Medical Systems and GE HealthCare; advisor for the EU Horizon 2020 LifeChamps project (875329) and the EU IHI Project IMAGIO (101112053); member of the *Radiology: Artificial Intelligence* trainee editorial board (2024–2026). **P.S.** No relevant relationships. **L.H.** No relevant relationships. **S.M.N.** Invited speaker for Bracco, Canon Medical, and Guerbet, received payment or honoraria; German Roentgen Society leadership board medical studies. **D.P.** No relevant relationships. **M.R.M.** No relevant relationships. **H.J.W.L.A.** No relevant relationships. **A.Z.** No relevant relationships. **L.C.A.** Member of the *Radiology: Artificial Intelligence* trainee editorial board (2023–2025).

References

1. Bennett CC, Hauser K. Artificial intelligence framework for simulating clinical decision-making: a Markov decision process approach. Artif Intell Med 2013;57(1):9–19.
2. Giada F, Bertaglia E, Reimers B, Noventa D, Raviele A. Current and emerging indications for implantable cardiac monitors. Pacing Clin Electrophysiol 2012;35(9):1169–1178.
3. Yi X, Adams SJ, Henderson RDE, Babyn P. Computer-aided assessment of catheters and tubes on radiographs: How good is artificial intelligence for assessment? Radiol Artif Intell 2020;2(1):e190082.
4. Raatikainen MJP, Arnar DO, Zeppenfeld K, Merino JL, Kuck K-H, Hindricks G. Current trends in the use of cardiac implantable electronic devices and interventional electrophysiological procedures in the European Society of Cardiology member countries: 2015 report from the European Heart Rhythm Association. Europace 2015;17(Suppl 4):iv1–iv72.
5. Kotalczyk A, Kalarus Z, Wright DJ, Boriani G, Lip GYH. Cardiac Electronic Devices: Future Directions and Challenges. Med Devices (Auckl) 2020;13:325–338.
6. Roth GA, Mensah GA, Johnson CO, et al; GBD-NHLBI-JACC Global Burden of Cardiovascular Diseases Writing Group. Global Burden of Cardiovascular Diseases and Risk Factors, 1990-2019: Update From the GBD 2019 Study. J Am Coll Cardiol 2020;76(25):2982–3021. [Published correction appears in J Am Coll Cardiol 2021;77(15):1958-1959.]
7. Jacob S, Shahzad MA, Maheshwari R, Panaich SS, Aravindhakshan R. Cardiac rhythm device identification algorithm using X-Rays: CaRDIA-X. Heart Rhythm 2011;8(6):915–922.
8. Neuenschwander JF, Peacock WF, Migeed M, et al. Safety and efficiency of emergency department interrogation of cardiac devices. Clin Exp Emerg Med 2016;3(4):239–244.
9. Howard JP, Fisher L, Shun-Shin MJ, et al. Cardiac Rhythm Device Identification Using Neural Networks. JACC Clin Electrophysiol 2019;5(5):576–586.
10. Chudow JJ, Jones D, Weinreich M, et al. A Head-to Head Comparison of Machine Learning Algorithms for Identification of Implanted Cardiac Devices. Am J Cardiol 2021;144:77–82.
11. Weinreich M, Chudow JJ, Weinreich B, et al. Development of an Artificially Intelligent Mobile Phone Application to Identify Cardiac Devices on Chest Radiography. JACC Clin Electrophysiol 2019;5(9):1094–1095.
12. Theriault Lauzier P, Gomes DG, Weng W, et al. Detection and identification of cardiac implanted electronic devices in a large data set of chest radiographs using semi-supervised artificial intelligence methods. Heart Rhythm 2023;20(4):642–643.
13. Kim UH, Kim MY, Park EA, et al. Deep Learning-Based Algorithm for the Detection and Characterization of MRI Safety of Cardiac Implantable Electronic Devices on Chest Radiographs. Korean J Radiol 2021;22(11):1918–1928.
14. Heart-devices. GitHub. github.com/AndreasZhukov/cied. Published 2024. Accessed June 2, 2024.
15. 3D Slicer image computing platform. 3DSlicer. https://www.slicer.org. Accessed July 18, 2023.
16. Wickham H, Averick M, Bryan J, et al. Welcome to the Tidyverse. J Open Source Softw 2019;4(43):1686.
17. Robin X, Turck N, Hainard A, et al. pROC: an open-source package for R and S+ to analyze and compare ROC curves. BMC Bioinformatics 2011;12(1):77.
18. Kuhn M. Building Predictive Models in R Using the caret Package. J Stat Softw 2008;28(5):1–26.
19. R: A language and environment for statistical computing. R-Team. https://www.R-project.org. Accessed July 18, 2023.